IEEE Access
Multidisciplinary | Rapid Review | Open Access Journal

Received 4 October 2022, accepted 20 October 2022, date of publication 25 October 2022, date of current version 2 November 2022.

Digital Object Identifier 10.1109/ACCESS.2022.3216889

RESEARCH ARTICLE

Design of a Six-Port Compact UWB MIMO Antenna With a Distinctive DGS for Improved Isolation

PRAVEEN KUMAR[1], SAMEENA PATHAN[2], OM PRAKASH KUMAR[1], SHWETA VINCENT[3], YASHWANTH NANJAPPA[1], (Senior Member, IEEE), PRADEEP KUMAR[4], PRANAV SHETTY[1], AND TANWEER ALI[1], (Senior Member, IEEE)

[1]Department of Electronics and Communication, Manipal Institute of Technology, Manipal Academy of Higher Education, Manipal 576104, India
[2]Department of Information and Communication Technology, Manipal Institute of Technology, Manipal Academy of Higher Education, Manipal 576104, India
[3]Department of Mechatronics, Manipal Institute of Technology, Manipal Academy of Higher Education, Manipal 576104, India
[4]Discipline of Electrical, Electronic and Computer Engineering, University of KwaZulu-Natal, Durban 4041, South Africa

Corresponding author: Tanweer Ali (tanweer.ali@manipal.edu)

ABSTRACT A low-profile printed six-port ultrawideband (UWB) antenna with a novel decoupling structure for enhancing port-to-port isolation is analyzed in this paper. Six symmetrical pyramidal form UWB antennas with defective ground structures interspersed with parasitic components served as a unique decoupling structure in the proposed design. The grounded branches and modified rectangular stubs on the ground plane generate closed and open current distribution channels, causing the uniform current flow to be disrupted and the coupling effect to be neutralized. The projected six-port antenna has an electrical dimension of $0.68 \times 0.89 \times 0.01\ \lambda^3$ (λ is computed using a lower frequency of 2.9 GHz), having a below -10 dB impedance bandwidth of 116% from 2.9 to 11 GHz. Across the impedance bandwidth, the average port-to-port isolation is better than 20 dB. The antenna design has acceptable radiation properties with a peak gain of 8.3 dBi at a frequency of 7.5 GHz. Further, the projected design is also exposed to the time domain characteristics and diversity metrics. Among the different ports, the values of the group delay and fidelity factors are less than 1.5 ns and more than 0.92, correspondingly. The values of the diversity parameters such as ECC < 0.075, DG approximately 10 dB, MEG<-3dB, TARC<-10 dB, CCL < 0.3 bps/Hz, and ME<-2 dB ensure that the projected design is appropriate for the MIMO applications. The designed antenna is fabricated and measured, and the results are in line with the simulation.

INDEX TERMS Isolation, antenna, decoupling structure, time-domain, ECC, DGS.

I. INTRODUCTION

The technological evolution makes electronic gadgets more innovative, compact, and portable. Multiple features on these devices require a wireless communication system with a high data rate and channel capacity. Ultrawideband (UWB) systems offer higher bandwidth and data rates [1]. The allowable transmission power of the UWB system is confined to 75 nW/MHz. The low power restricts the transmission to short-range communication, tracking, positioning, and radar applications [2], [3], [4]. The UWB provides various advantages; however, it suffers from multipath fading due to the dispersion of short input pulses. To efficiently utilize the UWB system's broader bandwidth, the multipath fading issue is resolved by incorporating the multiple input and multiple output (MIMO) technology. The MIMO technology in wireless communication helps overcome multipath fading and utilizes a multi-scattering atmosphere with no additional power and bandwidth. The monopole patch antennas are the most desirable antenna in the UWB MIMO system due to their nay advantages [5]. The aforementioned MIMO technology characteristics may be attained only

The associate editor coordinating the review of this manuscript and approving it for publication was Tutku Karacolak.

when the radiators of multiport antenna should have strong isolation structures that effectively mitigate the near-field coupling.

The literature divulges the different ways of designing UWB monopole antenna structures using conventional rectangular and circular patches [5]. The conventional patches are modified by carving or adding additional conducting material on radiating and ground planes. The idea behind increasing bandwidth is engraving slot, slit, stub structures on the radiator, and full/partial plane correspondingly such that these structures disturb the uniform current flow and improve the bandwidth. Different approaches for improving isolation in MIMO systems include embedding the matching network between antennas, metamaterial loading, parasitic element loading, neutralization line, and combining these techniques as a hybrid approach [6], [7], [8], [9], [10], [11]. Polarization diversity techniques are exploited by placing the antennas in orthogonal orientation with the parasitic elements loaded on the defected ground structure (DGS), as demonstrated in [12], to improve isolation. In [13], a low-pass filter is included between the elements to filter out the coupling effect. A compact UWB MIMO with spiral structure DGS is used to achieve enhanced isolation [14]. A reflector of a circular structure is loaded onto the radiator and connected to the DGS using vias to enhance isolation, as illustrated in [15]. A circular with tapered feedline UWB monopole antenna is duplicated to develop a two-port MIMO antenna [16]. The isolation is increased by inserting a stub between the elements and the vertical branch in DGS. The isolation among the fractal UWB antennas is achieved by positioning them perpendicular to each other [17].

This communication presents a distinctive decoupling structure to improve isolation among the six-port UWB MIMO antenna having a common ground plane. For a broader bandwidth, impedance matching is achieved by carving a pyramidal structure with a 1.8 mm vertical rectangle on the radiator and partial ground plane. The six-port MIMO antenna is formed by placing three UWB monopole antennas side by side, and this configuration is mirrored with horizontal reference. The inter-element separation is less than 1/4 λ, where the frequency of 2.9 GHz determines λ. The projected design exhibit S11 below -10 dB from 2.9 to 11.2 GHz and average isolation better than 20 dB throughout the operating frequency. The isolation is improved by employing parasitic elements on a defective ground structure (DGS), which results in a one-of-a-kind decoupling structure. Further, the projected design is exploited for analyzing time domain and MIMO diversity characteristics. For experimental validation, the proposed design is printed on an FR4 substrate ($\varepsilon_r = 4.4, \tan\delta = 0.02,$ and $h = 1.6mm$). The remaining work is structured as follows- an antenna design is described in section 2. Section 3 discusses the design and analysis of the decoupling structure. The outcome of the presented six-port antenna design and performance comparison with the previous work is portrayed in section 4. Section 5 depicts the concluding remarks.

II. SIX-PORT UWB MIMO ANTENNA DESIGN

A UWB monopole antenna with pyramidal and rectangular hybrid geometry as a radiation patch, a microstrip feedline, and a partial ground plane is presented in Figure 1, and geometrical parameters are listed in Table 1. An FR4 substrate having physical dimensions of $0.30 \times 0.22 \times 0.01\ \lambda^3$ (λ is computed using a lower frequency of 2.9 GHz) is employed to simulate the UWB antenna. The ground plane alteration influences the transmission line characteristics, resulting in a lower quality factor and greater operational bandwidth. The difference in ground plane length (g1) substantially affects the reflection coefficient curve, particularly changing the lower resonance frequency, as illustrated in Figure 2a. The increase in width of the rectangle (a3) does not affect the lower resonance frequency, but the higher resonance shifts towards the lower frequency, as shown in Figure 2b.

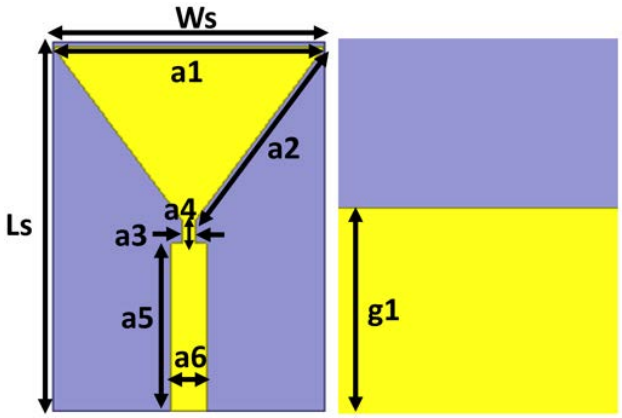

FIGURE 1. Schematic of the UWB antenna: radiating plane (left) and ground plane (right).

TABLE 1. Geometrical parameters of the UWB antenna (mm).

Ls	Ws	a1	a2	a3	a4	a5	a6	g1
31.5	23	22.5	18.4	1	1.9	14.3	3	17

The simulated UWB antenna is replicated side by side with the inter-element separation of 0.12λ (s1=13mm) from edge to edge. This configuration is parallelly mirrored at a distance of 0.08λ (s2=9mm) to construct a six-element MIMO antenna operating in the UWB band, as represented in Figure 3a. The optimal values of S1 and S2 are chosen by performing the parametric analysis. The horizontal and vertical inter-element spacing is less than a quarter wavelength, resulting in strong coupling between the MIMO elements. Figure 3b depicts the scattering parameter curves. Figure 3b demonstrates the poor reflection and transmission coefficient values caused by inappropriate impedance matching. The close proximity among elements causes low isolation, and the same can be witnessed by the current distribution plot, as represented in Figure 3c. The coupling effect of the excited antenna has a significant effect on the adjacent element.

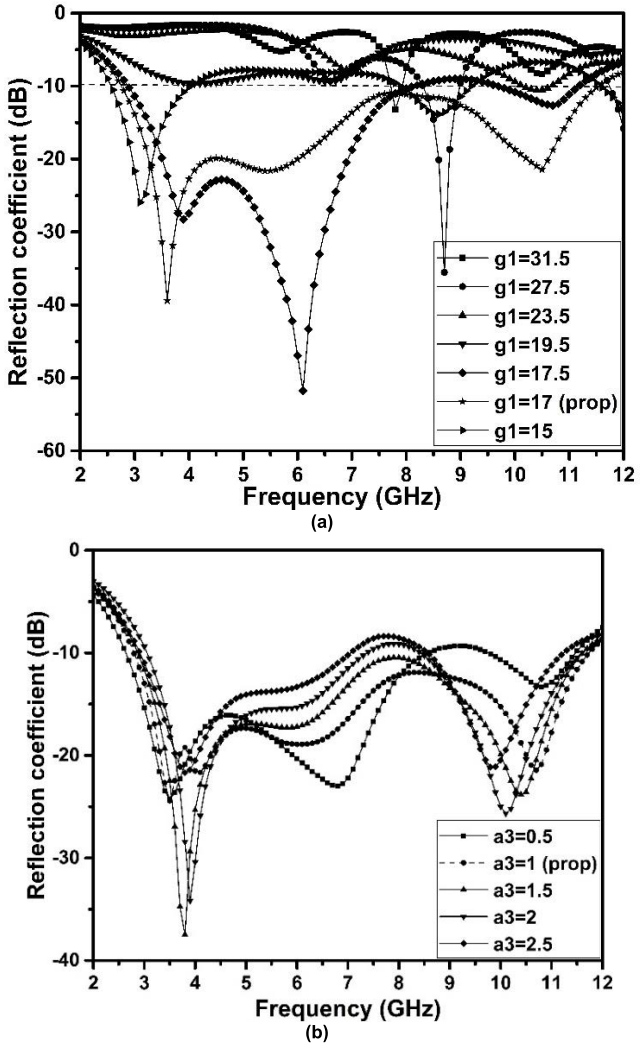

FIGURE 2. The effect of parameter variation on the reflection coefficient curve (a) g1, and (b) a3.

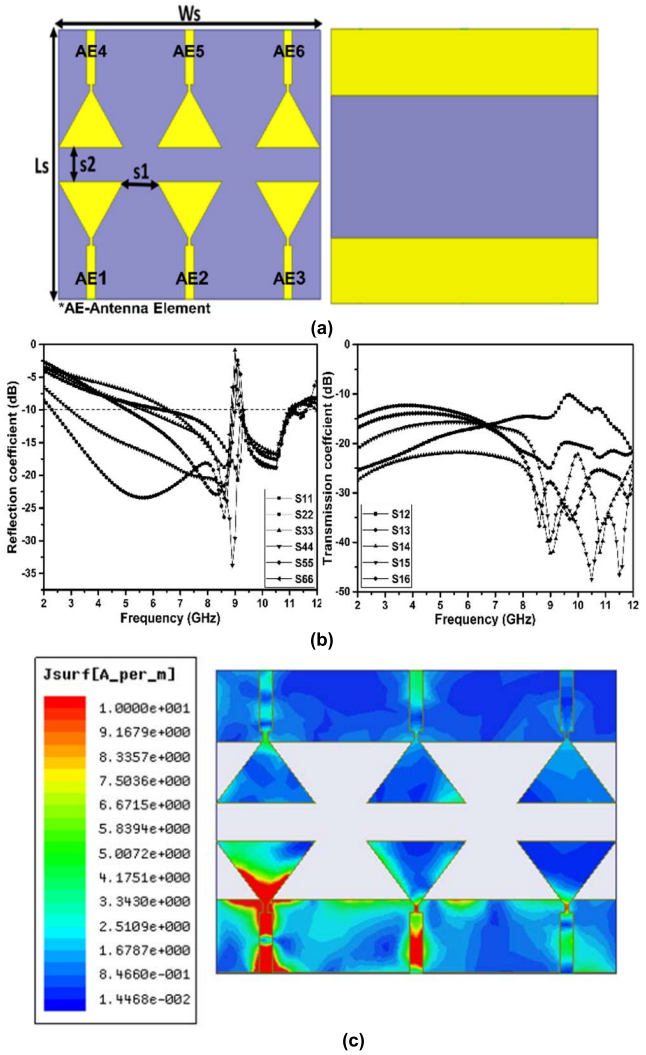

FIGURE 3. The MIMO antenna (a) Schematic of the MIMO antenna without decoupling structure, (b) S-parameters of the design, and (c) current distribution plot at 5GHz, depicting the mutual coupling.

The parasitic elements are embedded on the DGS to negate the inter-element coupling effect, as shown in Figure 4. The gap and conducting branches on the DGS attract the coupling field, resulting in the formation of a new local current channel with essentially no current coupling to the neighbouring elements. The projected six-port MIMO antenna has physical dimensions of $0.68 \times 0.89 \times 0.01\ \lambda^3$ (λ is computed using a lower frequency of 2.9 GHz) with an impedance bandwidth of 116 % of the center frequency ranging from 2.9 to 11 GHz. The insertion of unique DGS as a decoupling structure provides the average isolation better than the 20 dB over the operational frequency. The detailed physical dimensions are listed in Table 2.

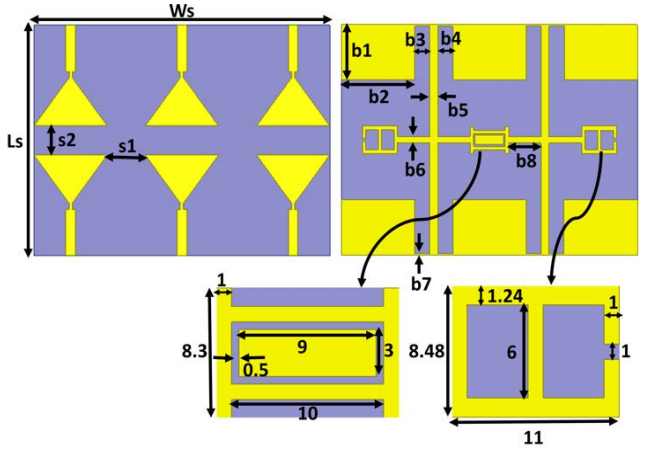

FIGURE 4. The Schematic of the projected six-port UWB MIMO antenna: radiating plane (left) and ground plane (right) (dimensions in mm).

III. DESIGN AND ANALYSIS OF DECOUPLING STRUCTURE

In order to accomplish a compact six-port antenna, three UWB monopole antennas are positioned next to each other and mirrored horizontally with the shared ground plane, as illustrated in Figure 4. The evolution of the decoupling structure and their S12 is depicted in Figures 5 and 6. The first step was initiated by extending a single element's ground

TABLE 2. Geometrical parameters of the UWB antenna (mm).

Ls	Ws	b1	b2	b3	b4	b5	b6	b7	b8	s1	s2
71	93	17	23	4.8	4.8	2.5	2	0.5	10.2	13	9

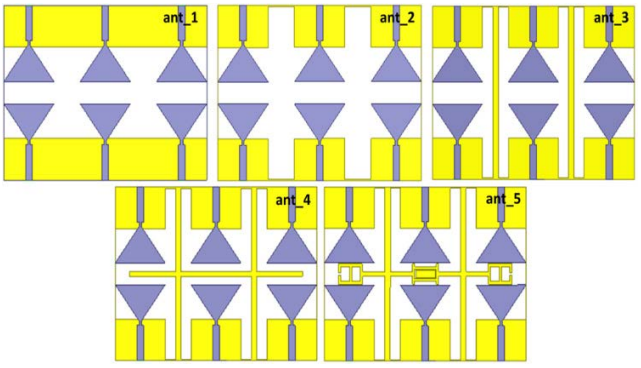

FIGURE 5. The evolution of decoupling structure to improve the isolation of six-port UWB antenna.

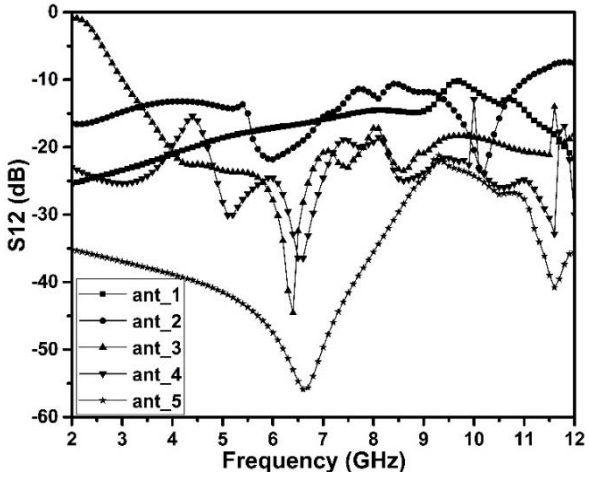

FIGURE 6. The simulated S21 of the ant_1, ant_2, ant_3, ant_4, ant_5.

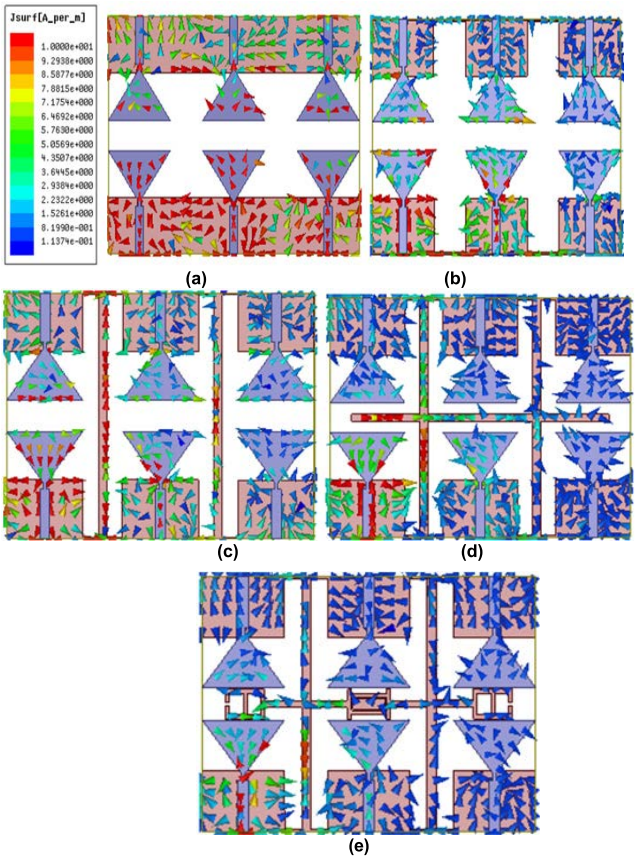

FIGURE 7. The simulated surface current flow plots at 9 GHz (a) ant_1, (b) ant_2, (c) ant_3, (d) ant_4, and (e) ant_5.

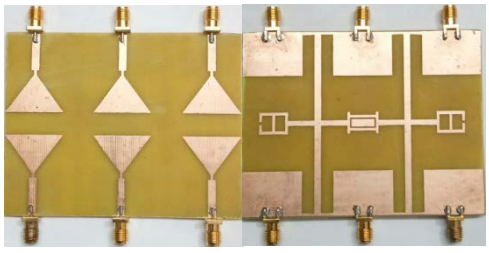

FIGURE 8. The Photographs of the top (left) and bottom (right) of the projected UWB MIMO antenna.

plane, as in ant_1 of Figure 5. The inter-element coupling influences the impedance matching and leads to poor isolation, especially at high frequencies. A pair of rectangular slots of 16.5×12 mm^2 is patterned in the ground plane as in ant_2 of Figure 5. In comparison to the previous step, the slots disrupt the uniform current distribution and improve isolation. Two verticles and horizontal branches are implanted consecutively in the DGS, as indicated in ant_3 and ant_4 of Figure 5. These branches combine to create an open and closed current flow path, resulting in a local alternative current channel. This local current path cancels out the coupling effect between the neighboring components. Further isolation is enhanced by embedding the parasitic elements into the modified DGS as in ant_5 of Figure 5. This arrangement provides average isolation better than the 20 dB among all ports by suppressing the coupling effect. The total physical dimensions of the parasitic elements are less than the half-wavelength (1/2 λ). Adjusting the relative length and position of the grounded branches and incorporating the modified rectangular stub and slot combination on the DGS improves the overall isolation throughout the operating bandwidth.

A. DECOUPLING MECHANISM

The decoupling process is investigated through the vector surface current distribution plots, as portrayed in Figure 7. One element is stimulated, and all other elements are terminated in the UWB MIMO antenna. The surface current in Figure 7a signifies the strong port-to-port coupling effect. The current distribution on the ground plane is disturbed

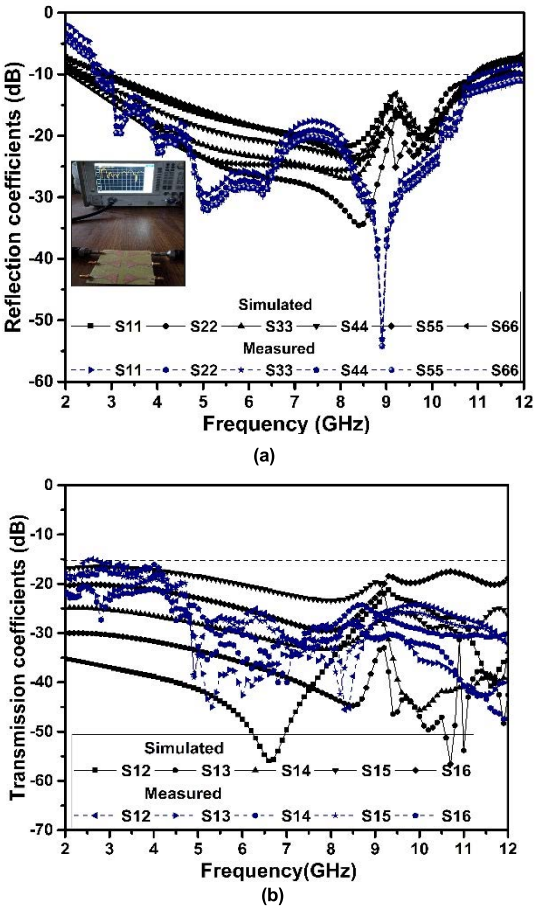

FIGURE 9. The scattering parameters graphs (a) reflection coefficient (b) transmission coefficient.

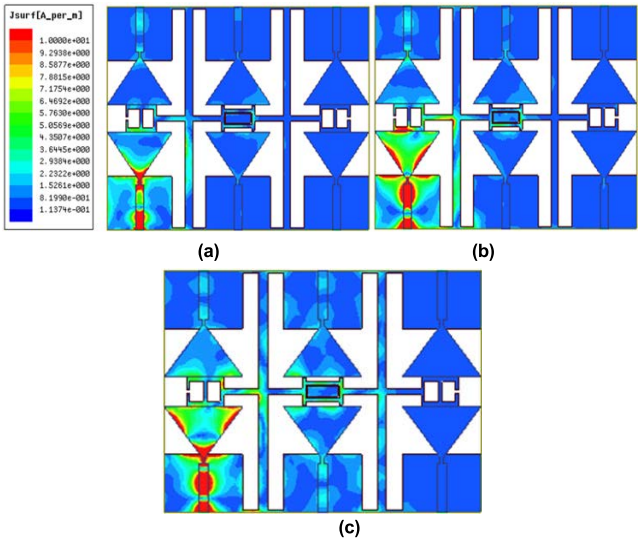

FIGURE 10. The simulated current distribution graphs (a) 5 GHz, (b) 7GHz, and (c) 9 GHz.

using a rectangular slot, two verticles, and horizontal ground branches with the embedding of the parasitic elements,

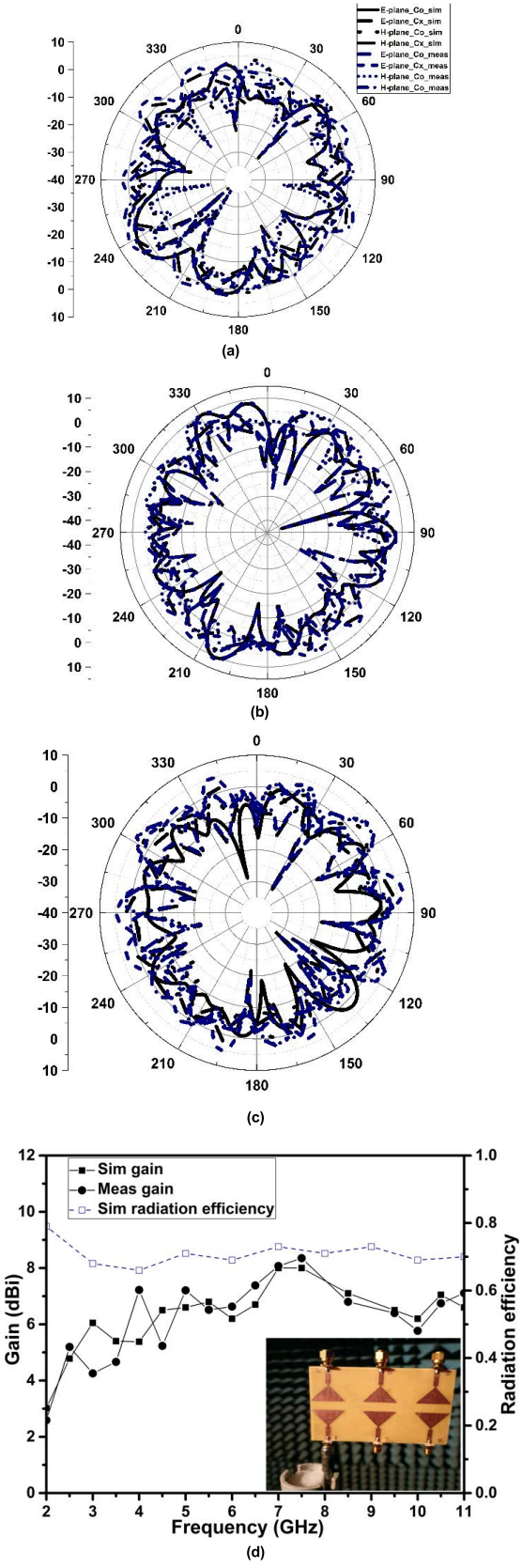

FIGURE 11. The simulated and measured radiation pattern at (a) 5 GHz, (b) 7 GHz, (c) 9 GHz, and (d) gain, radiation efficiency vs. frequency plot.

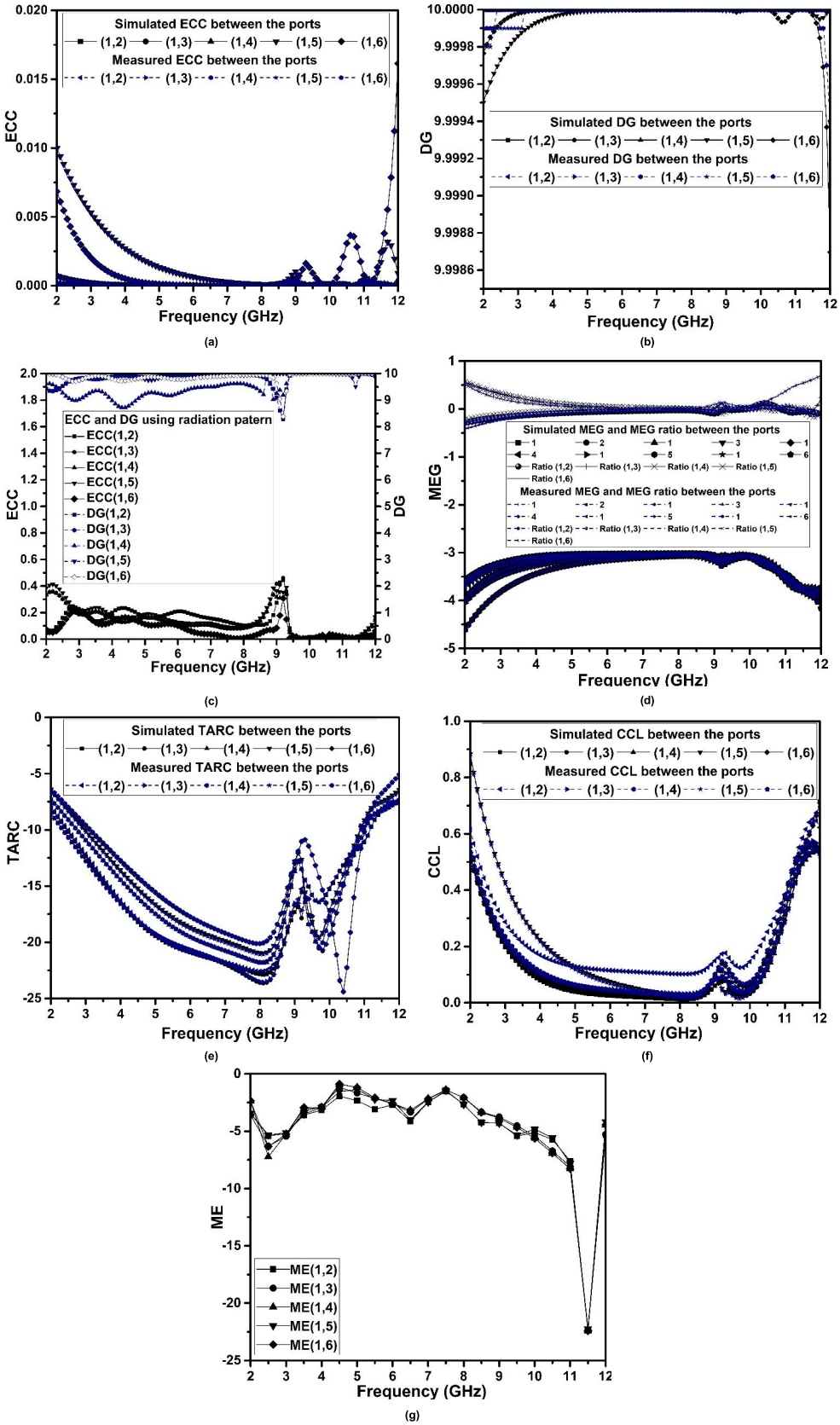

FIGURE 12. Plots of MIMO diversity parameters (a) ECC (s-parameters), (b) DG (s-parameters), (c) ECC and DG (radiation pattern), (d) MEG, (e) TARC, (f) CCL, and (g) ME.

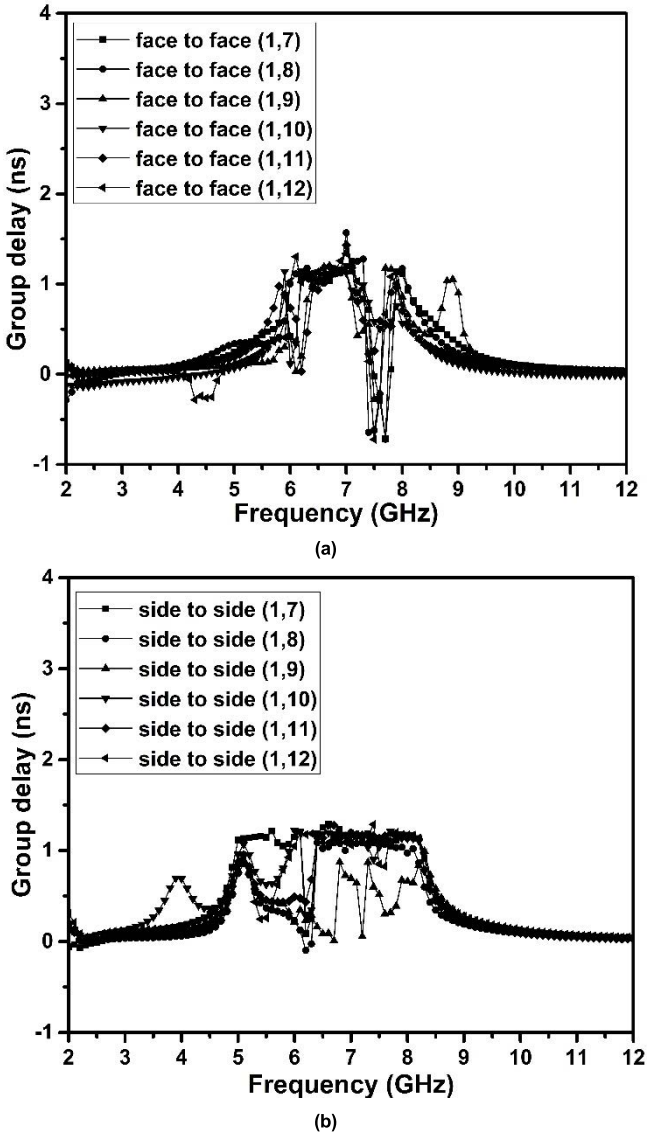

FIGURE 13. Normalized input and output pulses (a) side-to-side, (b) face-to-face configurations.

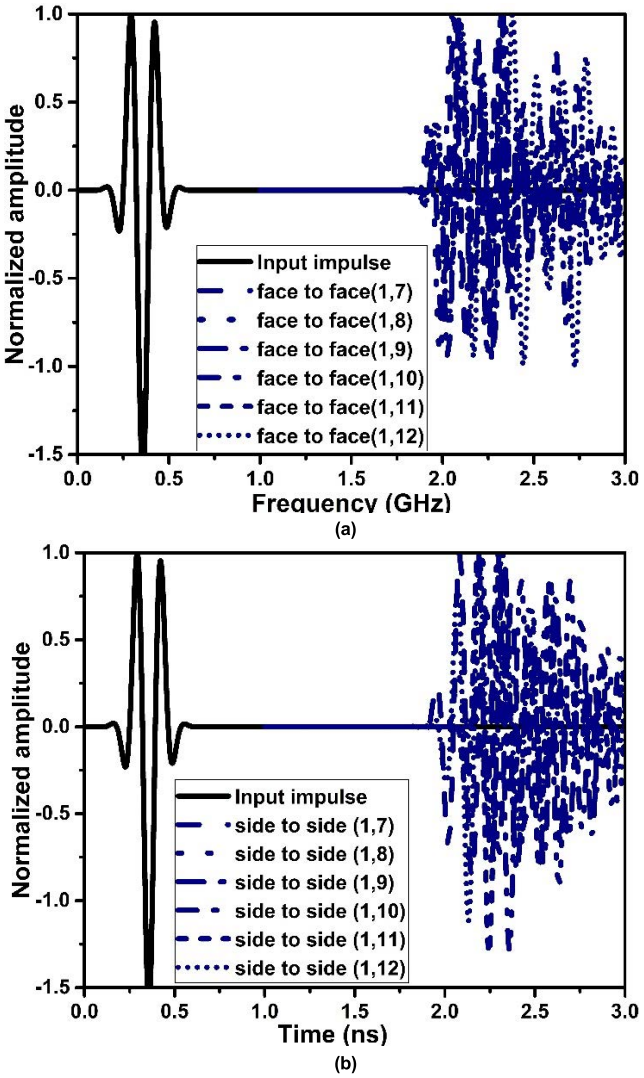

FIGURE 14. The designed antenna group delay (a) face-to-face (b) side-to-side configurations.

as represented in Figure 7b-e. Figure 7e signifies the direction of current flow in the stimulated antenna is steady and neighboring elements have opposite directions. The reverse current creation is caused by the DGS decoupling structure, which also reduces the coupling effect. Furthermore, the current on the DGS is higher, minimizing mutual coupling caused by ground surface oscillations. As a result, the decoupling structure shown here may effectively minimize antenna coupling.

IV. RESULTS AND DISCUSSION

Fabricating and testing the six-port UWB antenna (ant 5) validates the presented decoupling arrangement for the UWB MIMO antenna. Figure 8 illustrates a photograph of the presented UWB MIMO. The horizontal and verticle edge-to-edge spacings are 0.12λ and 0.08λ, respectively.

A. SCATTERING PARAMETERS

The scattering parameter graphs for the intended six-port antenna are illustrated in Figure 9. The data show that the simulated and measured results are consistent, with an acceptable margin of error owing to fabrication, soldering, and testing equipment tolerance. Figure 9a signifies the measured impedance bandwidth of 3 to 11.2 GHz. Figure 9b indicates the port-to-port isolation of the projected design. The modified ground plane, along with the insertion of ground branches and parasitic elements, provides the isolation of better than 20 dB throughout the impedance bandwidth (except for lower frequency 2.9 to 4 GHz).

B. CURRENT DISTRIBUTION

Figure 10 depicts the surface current distribution with the combination of DGS and parasitic elements as a decoupling structure at resonance frequencies of 5 GHz, 7 GHz, and 9 GHz to better articulate the influence of the decoupling

TABLE 3. Performance comparison of projected design with the existing designs.

Ref	Techniques used	Dimension (mm^3)	No. of elements	Impedance bandwidth (GHz)	Peak gain	Isolation (dB)	ECC (S-parameter/ 3D pattern)	DG	MEG	TARC	CCL	ME
24	Low pass and band pass filter and Vertical polarization	78×78×1.6	4	2.1-10	4.94 dBi	>13	NA / <0.17	>9.85	-	-	-	-
25	DGS and Polarization diversity	40×40×1.6	4	3-13.5	Average 4.5 dBi	>15	NA /<0.4	>9.95	-	-	<0.2	<-1
26	Coplanar waveguide (CPW), DGS	80×80×1.6	4	2.1-20	5.8 dB	>25	<0.02 / NA	≈10	-	<-10	<0.4	-
27	DGS and orthogonal	64×64×1.6	4	2.08-10.4	9.57 dBi	>20	NA / <0.15	>9.2	-3	-	<0.3	-
28	Parasitic element and orthogonal	50×50×1.6	4	2.4-18	5 dBi	>30	<0.0002/ NA	9.9	-	<-10	<0.2	-
29	asymmetric coplanar strip and orthogonal	48×52×1.6	4	2.7-11	Average 3.5 dBi	>20	<0.008/ NA	9.97	-	-	<0.4	<-1
30	CPW and orthogonal	81×87×1.6	4	3.03-10.74	7.9 dBi	>20	NA / <0.2	-	-	-	-	-
31	Vertical polarization	50×50×1.6	4	2-12	3.15 dBi	>17	NA / <0.15	-	-	-	-	-
Proposed	DGS and Parasitic element	71×95×1.6	6	2.9-11	8 dBi	>20	<0.075 / 0.4	≈10	<-3	<-10	<0.3	<-2

*- NA--not available

structure. The decoupling structure blocks the coupling current from port 1 to other ports.

C. RADIATION CHARACTERISTICS

The 2D radiation pattern is presented using simulated and measured data for the resonant frequencies of 5GHz, 7GHz, and 9GHz, as shown in Figure 11a-c. The radiation pattern of the designed antenna is determined by stimulating one port and disconnecting all other ports with the matching condition at the xz and yz planes. The antenna exhibits the quasi omnidirectional pattern at the resonating frequencies. The simulated and measured gain versus frequency plot of the designed antenna is represented in Figure 11d. The minimum and maximum gain of 4.2 dBi and 8.3 dBi are observed at frequencies of 3.5 GHz and 7.5 GHz, respectively.

D. DIVERSITY CHARACTERISTICS

The envelope correlation coefficient (ECC), diversity gain (DG), mean effective gain (MEG), total active reflection coefficient (TARC), channel capacity loss (CCL), and multiplexing efficiency (ME) are tested on the projected six-port UWB MIMO antenna. The aforementioned metrics are determined using measured data and MATLAB to ensure consistency with the simulated outcomes. The ECC characterizes the amount of correlation among the antenna elements. The ECC can be computed using a 3D radiation pattern and as well using S-parameters for the antenna having high efficiency. The signal to interference strength is defined by the DG and is estimated using ECC. The MEG gives the antenna's average power ratio radiated to incident relative to the isotropic environment. TARC provides information on the overall power radiated to the total incident power in the multiport microwave devices. The CCL determines the losses that occur during the transmission of data. It specifies the maximum channel transmission rate required for unwavering communication. To assess the performance of the MIMO antenna, the ME is calculated by analyzing the correlation between the elements and their efficiencies. For the two-port antenna, diversity parameters are calculated using the equations reported in [18], [19], [20], and [21].

The designed antenna exhibit ECC of 0.075 (s-parameter) and 0.4 (radiation pattern), DG approximately 10 dB (s-parameter) and >9 dB (radiation pattern), MEG <-3 dB, TARC<-10 dB, CCL <0.3 bps/Hz, and ME <-2 dB as illustrated in the Figure 12. These characteristics ensure that the designed antenna is appropriate for MIMO applications.

E. TIME DOMAIN CHARACTERISTICS

The time-domain metrics group delay (GD) and fidelity factor (FF) are examined for the designed antenna. To perform time-domain analysis, identical antennas are arranged 100 mm apart in a face-to-face and side-to-side configuration [22], [23]. The transmitted and received pulse qualities can be studied in order to ensure seamless communication. GD describes the phase linearity among the input and output signals. Analytically GD is the derivative function of phase response to the angular frequency as defined in the below

equation 1.

$$\tau_g(\omega) = -\frac{d\varphi(\omega)}{d\omega} \tag{1}$$

The phase difference between the ports is characterized by φ. The group delay of the designed antenna is less than 1.5 ns, as illustrated in Figure 13.

The FF is another important statistic that specifies the level of correlation between the incoming and outgoing pulse forms. The FF is calculated using the normalized transmitted and received pulses as in equations 2-4 [12].

$$T_s^n = \frac{T_s(t)}{\sqrt{\int_{-\infty}^{\infty} |T_s(t)|^2 \, dt}} \tag{2}$$

$$R_s^n = \frac{R_s(t)}{\sqrt{\int_{-\infty}^{\infty} |R_s(t)|^2 \, dt}} \tag{3}$$

$$FF = \max \int_{-\infty}^{\infty} T_s^n(t) \, R_s^n(t+\tau) dt \tag{4}$$

Normalization is performed to ensure that only the signal pattern is examined instead of its amplitude. The normalized input and output pulses are represented in Figure 14. The consistency among transmitted and received impulses are determined using the FF equation. In both configurations, FF is found to be greater than 0.92. The estimated fidelity factor values ensure that the pulse received at the receiver has as little interference as possible.

F. COMPARATIVE ANALYSIS

The effectiveness of the projected design performance is evaluated by comparing it to existing UWB MIMO antenna designs in the literature, as illustrated in Table 3. The proposed design outperforms the physical dimension, MIMO diversity features, and time-domain characteristics.

V. CONCLUSION

This paper describes an innovative decoupling structure design for identical six-port antennas with impedance bandwidths ranging from 2.9 to 11 GHz. The S11 curve, isolation, radiation properties, MIMO diversity parameters, and time-domain aspects of the designed antenna are all examined. The unique decoupling structure consisting of DGS with grounded branches and rectangular pattern parasitic elements minimizes the inter-element coupling effect. The impedance discontinuity at the ground plane suppresses the coupling effect. The average port-to-port decoupling of the six-port UWB antenna is greater than 20 dB over the impedance bandwidth of 2.9 to 11 GHz. Likewise, the proposed structure is subjected to time-domain features and diversity metrics. The group delay and fidelity factors values among the different ports are less than 1.5 ns and greater than 0.92, respectively. The MIMO diversity parameters ECC < 0.075, DG ≈ 10 dB, MEG<-3dB, TARC<-10 dB, CCL < 0.3 bps/Hz, and ME<-2 dB. Finally, the designed antenna structure is compared to the prior UWB MIMO antennas. All performance metrics are acceptable, and the proposed antenna is a viable contender for UWB communication systems.

REFERENCES

[1] M. G. N. Alsath and M. Kanagasabai, "Compact UWB monopole antenna for automotive communications," *IEEE Trans. Antennas Propag.*, vol. 63, no. 9, pp. 4204–4208, Sep. 2015.
[2] E. M. Staderini, "UWB radars in medicine," *IEEE Aerosp. Electron. Syst. Mag.*, vol. 17, no. 1, pp. 13–18, Jan. 2002.
[3] B. Sobhani, E. Paolini, A. Giorgetti, M. Mazzotti, and M. Chiani, "Target tracking for UWB multistatic radar sensor networks," *IEEE J. Sel. Topics Signal Process.*, vol. 8, no. 1, pp. 125–136, Feb. 2014.
[4] R. S. Kshetrimayum, "An introduction to UWB communication systems," *IEEE Potentials*, vol. 28, no. 2, pp. 9–13, Mar. 2009.
[5] P. Kumar, M. M. M. Pai, and T. Ali, "Design and analysis of multiple antenna structures for ultrawide bandwidth," *Telecommun. Radio Eng.*, vol. 80, no. 6, pp. 41–53, 2021.
[6] R. Gurjar, D. K. Upadhyay, B. K. Kanaujia, and A. Kumar, "A compact modified Sierpinski carpet fractal UWB MIMO antenna with square-shaped funnel-like ground stub," *AEU-Int. J. Electron. Commun.*, vol. 117, Apr. 2020, Art. no. 153126.
[7] P. Kumar, T. Ali, and M. M. M. Pai, "A compact highly isolated two- and four-port ultrawideband multiple input and multiple output antenna with wireless LAN and X-band notch characteristics based on defected ground structure," *Int. J. Commun. Syst.*, vol. 35, no. 17, p. e5331, Nov. 2022.
[8] G. Bharti, D. Kumar, A. K. Gautam, and A. Sharma, "Two-port dual-band circularly polarized dielectric resonator-based MIMO antenna with polarization diversity," *Electromagnetics*, vol. 40, no. 7, pp. 463–478, Oct. 2020.
[9] P. Kumar, T. Ali, and M. P. Mm, "Characteristic mode analysis-based compact dual band-notched UWB MIMO antenna loaded with neutralization line," *Micromachines*, vol. 13, no. 10, p. 1599, Sep. 2022.
[10] D. Gao, Z.-X. Cao, S.-D. Fu, X. Quan, and P. Chen, "A novel slot-array defected ground structure for decoupling microstrip antenna array," *IEEE Trans. Antennas Propag.*, vol. 68, no. 10, pp. 7027–7038, Oct. 2020.
[11] P. Kumar, T. Ali, and M. M. M. Pai, "Electromagnetic metamaterials: A new paradigm of antenna design," *IEEE Access*, vol. 9, pp. 18722–18751, 2021.
[12] Z. Chen, W. Zhou, and J. Hong, "A miniaturized MIMO antenna with triple band-notched characteristics for UWB applications," *IEEE Access*, vol. 9, pp. 63646–63655, 2021.
[13] A. S. A. El-Hameed, M. G. Wahab, N. A. Elshafey, and M. S. Elpeltagy, "Quad-port UWB MIMO antenna based on LPF with vast rejection band," *AEU-Int. J. Electron. Commun.*, vol. 134, May 2021, Art. no. 153712.
[14] P. Kumar, T. Ali, and M. Pai, "Highly isolated ultrawideband multiple input and multiple output antenna for wireless applications," *Eng. Sci.*, vol. 17, pp. 83–90, Nov. 2021.
[15] A. Mohanty and S. Sahu, "Design of 8-port compact hybrid fractal UWB MIMO antenna with a conjoined reflector-ground integration for isolation improvement," *AEU-Int. J. Electron. Commun.*, vol. 145, Feb. 2022, Art. no. 154102.
[16] B. T. Ahmed and I. F. Rodríguez, "Compact high isolation UWB MIMO antennas," *Wireless Netw.*, vol. 28, no. 5, pp. 1977–1999, Jul. 2022.
[17] A. G. Alharbi, U. Rafique, S. Ullah, S. Khan, S. M. Abbas, E. M. Ali, M. Alibakhshikenari, and M. Dalarsson, "Novel MIMO antenna system for ultra wideband applications," *Appl. Sci.*, vol. 12, no. 7, p. 3684, Apr. 2022.
[18] M. S. Sharawi, A. T. Hassan, and M. U. Khan, "Correlation coefficient calculations for MIMO antenna systems: A comparative study," *Int. J. Microw. Wireless Technol.*, vol. 9, no. 10, pp. 1991–2004, Dec. 2017.
[19] S. H. Chae, S.-k. Oh, and S.-O. Park, "Analysis of mutual coupling, correlations, and TARC in WiBro MIMO array antenna," *IEEE Antennas Wireless Propag. Lett.*, vol. 6, pp. 122–125, 2007.
[20] A. A. Glazunov, A. F. Molisch, and F. Tufvesson, "Mean effective gain of antennas in a wireless channel," *IET Microw., Antennas Propag.*, vol. 3, no. 2, p. 214, 2009.
[21] M. S. Sharawi, "Current misuses and future prospects for printed multiple-input, multiple-output antenna system [wireless corner]," *IEEE Antennas Propag. Mag.*, vol. 59, no. 2, pp. 162–170, Apr. 2017.
[22] Q. V. D. Brande, S. Lemey, and H. Rogier, "Planar sectoral antenna for IR-UWB localization with minimal range estimation biasing," *IEEE Antennas Wireless Propag. Lett.*, vol. 20, no. 2, pp. 135–139, Feb. 2021.
[23] S. Khangarot, B. V. Sravan, N. Aluru, A. W. M. Saadh, R. Poonkuzhali, O. P. Kumar, T. Ali, and M. M. M. Pai, "A compact wideband antenna with detailed time domain analysis for wireless applications," *Ain Shams Eng. J.*, vol. 11, no. 4, pp. 1131–1138, Dec. 2020.

[24] B. Ramakrishnan and V. M. Sivashanmugham, "Novel four-port reconfigurable filtering MIMO antenna for multi-standard automotive communications," *AEU-Int. J. Electron. Commun.*, vol. 146, Mar. 2022, Art. no. 154108.
[25] A. A. Khan, S. A. Naqvi, M. S. Khan, and B. Ijaz, "Quad port miniaturized MIMO antenna for UWB 11 GHz and 13 GHz frequency bands," *AEU-Int. J. Electron. Commun.*, vol. 131, Mar. 2021, Art. no. 153618.
[26] V. S. D. Rekha, P. Pardhasaradhi, B. T. P. Madhav, and Y. U. Devi, "Dual band notched orthogonal 4-element MIMO antenna with isolation for UWB applications," *IEEE Access*, vol. 8, pp. 145871–145880, 2020.
[27] A. Mohanty and S. Sahu, "4-port UWB MIMO antenna with bluetooth-LTE-WiMax band-rejection and vias-MCP loaded reflector with improved performance," *AEU-Int. J. Electron. Commun.*, vol. 144, Feb. 2022, Art. no. 154065.
[28] R. R. Elsharkawy, A. S. A. El-Hameed, and S. M. El-Nady, "Quad-port MIMO filtenna with high isolation employing BPF with high out-of-band rejection," *IEEE Access*, vol. 10, pp. 3814–3824, 2022.
[29] A. A. Ibrahim and W. A. E. Ali, "High isolation 4-element ACS-fed MIMO antenna with band notched feature for UWB communications," *Int. J. Microw. Wireless Technol.*, vol. 14, no. 1, pp. 54–64, Feb. 2022.
[30] K. Srivastava, A. Kumar, B. K. Kanaujia, S. Dwari, and S. Kumar, "A CPW-fed UWB MIMO antenna with integrated GSM band and dual band notches," *Int. J. RF Microw. Comput.-Aided Eng.*, vol. 29, no. 1, Jan. 2019, Art. no. e21433.
[31] M. S. Khan, S. A. Naqvi, A. Iftikhar, S. M. Asif, A. Fida, and R. M. Shubair, "A WLAN band-notched compact four element UWB MIMO antenna," *Int. J. RF Microw. Comput.-Aided Eng.*, vol. 30, no. 9, Sep. 2020, Art. no. e22282.

PRAVEEN KUMAR received the B.E. degree in electronics and communication engineering and the M.Tech. degree in microelectronics and control systems from Visvesvaraya Technological University, Belagavi, Karnataka, India. He is currently pursuing the Ph.D. degree with the Department of Electronics and Communication Engineering, Manipal Institute of Technology, Manipal Academy of Higher Education, Manipal, India. His research interest includes microstrip antennas. He is a member of IETE, India.

SAMEENA PATHAN is currently working as an Assistant Professor with the Department of Information and Communication Technology, Manipal Institute of Technology, Manipal Academy of Higher Education, Manipal. Her research interests include pattern recognition, medical image analysis, artificial intelligence, and machine learning.

OM PRAKASH KUMAR is currently working as an Assistant Professor-Senior Scale with the Department of Electronics and Communication Engineering, Manipal Institute of Technology, Manipal Academy of Higher Education, Manipal. His research interest includes antenna design.

SHWETA VINCENT received the B.E. degree in electronics and communication engineering from Anna University, Chennai, India, in 2006, the M.Tech. degree in computer and communication engineering from Karunya University, Coimbatore, India, in 2010, and the Ph.D. degree in antenna design from the Karunya Institute of Technology and Sciences, Coimbatore, in 2020. She has been working as an Assistant Professor-Senior Scale with the Department of Mechatronics Engineering, Manipal Institute of Technology, Manipal Academy of Higher Education, Manipal, since 2015. She has published 20 articles in national and international journals/conference proceedings. Her research interests include antenna design, remote sensing, and machine learning.

YASHWANTH NANJAPPA (Senior Member, IEEE) received the B.E. degree in electronics and communication engineering from Visvesvaraya Technological University, Belagavi, in 2010, the M.Tech. degree in signal processing and VLSI from Jain University, Bengaluru, in 2012, and the Ph.D. degree from Visvesvaraya Technological University, in 2020. He is currently working as an Assistant Professor–Senior Scale with the Department of Electronics and Communication Engineering, Manipal Institute of Technology, Manipal Academy of Higher Education, Manipal. He has more than ten years of teaching experience for UG and PG students. He has authored or coauthored more than 15 research papers in international journals/conferences proceedings. He has five Indian/International patents published/granted. He has submitted research proposals to government agencies. His research interests include wireless sensor networks, signal processing, and communication systems and antennas. He is an Execom Member of the IEEE Mangalore Sub-Section, IEEE ComSoc Bangalore Section, and IEEE Young Professionals Bangalore Section for the year 2022. He is also an editorial board member/TPC/session chair/reviewer of many international journals/conferences. He has delivered many technical talks for faculties and students.

PRADEEP KUMAR received the bachelor's, Master of Engineering, and Doctor of Philosophy degrees in electronics and communication engineering, in 2003, 2005, and 2009, respectively. He completed his postdoctoral studies at the Autonomous University of Madrid, Spain. He is currently working with the University of KwaZulu-Natal, South Africa. He has over 15 years of experience in academics and research. He has held various positions, such as a Lecturer, a Senior Lecturer, an Assistant Professor, and an Associate Professor. He is the author of many research papers published in various peer-reviewed journals/conferences. His current research interests include antennas, antenna arrays, and wireless communications. He is registered as a Professional Engineer with the Engineering Council of South Africa. He received various awards/fellowships, such as an MHRD Fellowship, an A4U Fellowship, the Research Excellence Award, the J. W. Nelson Fund Research Award, and the CAES Research Award. He is serving as a Reviewer/a TPC Member for many journals/conferences, such as IEEE TRANSACTIONS ON ANTENNAS AND PROPAGATION, IEEE ACCESS, *Progress in Electromagnetics Research*, *ACES Journal*, IEEE SYSTEMS JOURNAL, *SAIEE Africa Research Journal*, the *International Journal of Electronics*, SATNAC, and IEEE Africon.

PRANAV SHETTY is currently pursuing the Graduate degree with the Department of Electronics and Communication Engineering, Manipal Institute of Technology, Manipal Academy of Higher Education, Manipal. His research interests include antenna design and wireless communication.

TANWEER ALI (Senior Member, IEEE) received the B.Tech. degree in E&C from Punjab Technological University, Punjab, in 2011, the M.E. degree in wireless communication from the Birla Institute of Technology, Mesra, Ranchi, in 2014, and the Ph.D. degree in antenna engineering, in March 2019. He is currently working as an Associate Professor with the Department of Electronics and Communication Engineering, Manipal Institute of Technology, Manipal Academy of Higher Education, Manipal. He is an active researcher in the field of microstrip antennas, wireless communication, and microwave imaging. He has been listed in top 2% scientists across the world for the year 2021 and 2022 by the prestigious list published by Stanford University, USA, indexed by Scopus. He has published more than 130 papers in reputed web of science (SCI) and Scopus indexed journals and conferences and has filled seven Indian patents, of which three have been published. He has more than 1371 citations with an H-index of 22 and i-10 index of 37. He is also guiding four regular Ph.D. students and five part-time Ph.D. students and is heading the antenna research group and laboratory at MIT. In 2020, he has received best Ph.D. thesis award from Board of IT Education (BITES), Karnataka. He has organized and is the Technical Programme Committee Chair of many reputed IEEE conferences, such as IEEE DISCOVER, IEEE ANTS, IEEE COMSNETS, IEEE TENCON, IEEE ICAECC, IEEE TEMSNET, and AICECS 2021. He is on the board of a Reviewer of journals, such as the IEEE Transactions on Antennas and Propagation, IEEE Antennas and Wireless Propagation Letters, IEEE Access, *IET Microwaves, Antennas and Propagation*, *IET of Electronics Letter*, *Wireless Personal Communications* (WPCs) (Springer), *AEU-International Journal of Electronics and Communications*, *Microwave and Optical Technology Letters* (MOTL) (Wiley), *International Journal of Antennas and Propagation* (Hindawi), *Advanced Electromagnetics*, *Progress in Electromagnetics Research* (PIER), *KSII Transactions on Engineering Science*, *International Journal of Microwave and Wireless Technologies*, *Frequenz*, *Radioengineering*, and IEEE Open Journal of Antennas and Propagation.